Water Research 149 (2019) 617–631

Contents lists available at ScienceDirect

Water Research

journal homepage: www.elsevier.com/locate/watres

Application of unstructured kinetic models to predict microcystin biodegradation: Towards a practical approach for drinking water treatment

Derek C. Manheim*, Russell L. Detwiler, Sunny C. Jiang

Department of Civil and Environmental Engineering, University of California, Irvine, CA, USA

ARTICLE INFO

Article history:
Received 6 July 2018
Received in revised form
20 October 2018
Accepted 7 November 2018
Available online 12 November 2018

Keywords:
Microcystin
Biodegradation
Biological filtration
Unstructured model
Monod kinetics
Parameter estimation

ABSTRACT

Biological drinking water treatment technologies offer a cost-effective and sustainable approach to mitigate microcystin (MC) toxins from harmful algal blooms. To effectively engineer these systems, an improved predictive understanding of the bacteria degrading these toxins is required. This study reports an initial comparison of several unstructured kinetic models to describe MC microbial metabolism by isolated degrading populations. Experimental data was acquired from the literature describing both MC removal and cell growth kinetics when MC was utilized as the primary carbon and energy source. A novel model-data calibration approach melding global single-objective, multi-objective, and Bayesian optimization in addition to a fully Bayesian approach to model selection and hypothesis testing were applied to identify and compare parameter and predictive uncertainties associated with each model structure. The results indicated that models incorporating mechanisms of enzyme-MC saturation, affinity, and cooperative binding interactions of a theoretical single, rate limiting reaction accurately and reliably predicted MC degradation and bacterial growth kinetics. Diverse growth characteristics were observed among MC degraders, including moderate to high maximum specific growth rates, very low to substantial affinities for MC, high yield of new biomass, and varying degrees of cooperative enzyme-MC binding. Model predictions suggest that low specific growth rates and MC removal rates of degraders are expected in practice, as MC concentrations in the environment are well below saturating levels for optimal growth. Overall, this study represents an initial step towards the development of a practical and comprehensive kinetic model to describe MC biodegradation in the environment.

1. Introduction

The quality of freshwater resources has become progressively challenged by the increasing frequency and severity of harmful cyanobacterial blooms (Paerl and Huisman, 2009; Paerl and Paul, 2012; O'Neil et al., 2012). Bloom events associated with toxic species of the *Microcystis*, *Anabaena*, *Planktothrix*, and *Nostoc* genera result in the release of biotoxins into receiving reservoirs or lake ecosystems (Huisman et al., 2006; Merel et al., 2013; Schmidt et al., 2014). The microcystin (MC) class of cyanobacterial toxins, composed of seven amino acids in a cyclical structure, are the most common and toxic in the environment. Over one hundred structural congeners of MC have been identified to date (Huisman et al., 2006; Puddick et al., 2014). MCs are both hepatotoxic and known human carcinogens, prompting the World Health Organization (WHO) and US EPA to develop guidelines for total MCs in drinking water of 1 μg/L (US EPA, 2015).

Of the broad class of MC toxins produced during cyanobacterial blooms, MC-LR (*L* and *R* standing for Leucine and Arginine, respectively, for two of the variable amino acids in the cyclical structure) is the most common and toxic (Edwards et al., 2009; Cheung et al., 2013). The high stability of the cyclical structure of MCs leads to their persistence in the environment and poses a human health threat through exposure to recreational and drinking water. Although conventional drinking water treatment technologies, such as coagulation, flocculation, and sedimentation can effectively remove intracellular MCs from source water, the extracellular fraction is sparingly removed (Westrick, 2008; Westrick et al., 2010). Advanced treatment technologies to remove total

---

* Corresponding author. Department of Civil and Environmental Engineering, University of California, Irvine, CA, 92617, USA.
E-mail address: dmanheim@uci.edu (D.C. Manheim).

https://doi.org/10.1016/j.watres.2018.11.014
0043-1354/© 2018 Elsevier Ltd. All rights reserved.

MCs from drinking water, such as granular activated carbon (GAC) or ozonation are effective, yet energy intensive, costly, and subject to some treatment variability (Westrick et al., 2010; Ho et al., 2012).

Bioremediation strategies, such as biological filtration (biofiltration), which specifically target the removal of MCs from drinking water, have advanced as a viable alternative (Li et al., 2011, 2012, 2015; Ho et al., 2007, 2012). Bio-based treatment strategies rely on the metabolism of MCs as auxiliary or sole carbon, energy, and nutrient (nitrogen) sources by microbial communities indigenous to the source water (Li et al., 2011, 2017; Ho et al., 2012). However, high variability in indigenous bacteria composition, temperature, pH, and the presence of exogenous nutrients pose formidable barriers to consistent removal of MC in these systems (Li et al., 2017).

To overcome these limitations and progress toward “engineered” bio-based MC remediation systems, an improved predictive understanding of MC biodegradation is required. A practical approach is to model MC biodegradation using existing theory from the fields of biochemical engineering, bioremediation, and wastewater treatment (Esener et al., 1983; Kovárová-Kovar and Egli, 1998; Alexander, 1999; Shuler and Kargi, 2002; Tchobanoglous et al., 2003; Okpokwasili and Neweke, 2006). Unstructured kinetic models (i.e., the Monod kinetic equation) to describe biodegradation in field and laboratory settings, have gained wide acceptance in applications ranging from the prediction of microbial degradation of contaminants in the environment to treatment system design (Simkins and Alexander, 1984; Rittmann et al., 1986; Suarez and Rifai, 1999; Al-Khalid and El-Naas, 2012; El-Naas et al., 2014). The popularity of unstructured kinetic models in these engineering applications stems from the avoidance of unnecessary complexity and computational burden associated with many structured models (Esener et al., 1983).

Despite the practicality of unstructured kinetic models, the great number of models available describing different growth mechanisms, uncertainty associated with parameter estimates, and difficulties arising from non-linear regression during model calibration often limit their use in an environmental context (Koch, 1982; Robinson, 1985; Grady et al., 1996; Kovárová-Kovar and Egli, 1998; Knightes and Peters, 2000). Of the number of challenges, identifying the mechanisms to include (i.e., the appropriate model) and arriving at accurate and reliable parameter estimates are primary issues undermining the predictive utility of unstructured kinetic models. For example, a broad range of unstructured model frameworks, from theoretical single, rate limiting enzyme catalyzed reactions (i.e., Monod, 1949) to those that account for transport and uptake of substrate (i.e., Powell, 1967), have been developed to describe microbial growth. In addition, reaching uncorrelated estimates of the maximum specific growth rate (μ_{max}) and half saturation constant (K_s) parameter values of many unstructured kinetic models has remained a well-known challenge over the years (Nihtilä and Virkkunen, 1977; Holmberg, 1982; Robinson and Tiejde, 1983; Liu and Zachara, 2001).

In this study, we address the following questions as a preliminary step toward the development of a practical and comprehensive MC biodegradation model in natural or engineered treatment systems. Importantly, we anticipate that the unstructured kinetic modelling framework reviewed herein will serve as a foundation for future modelling efforts focused on integrating more complex mechanisms to better reflect MC biodegradation in environmental settings:

1) What underlying mechanisms in existing unstructured kinetic growth model frameworks most reliably describe MC biodegradation kinetics?
2) What range in parameters (i.e., μ_{max}, K_s) are associated with these MC degrading organisms and how do they compare to other xenobiotic, micropollutant, or other organic chemical degrading organisms?
3) What is the relative level of confidence and certainty in the model predictions and estimated parameters?
4) Which parameters of these models are most sensitive, and can we identify any parameters that are non-influential?

In addressing these questions, we seek to compare the predictive performance of, and obtain reliable parameter estimates for, several unstructured kinetic models describing MC biodegradation. To this end, experimental data was mined from the literature describing growth and MC metabolism of various isolated degrading bacterial populations using MC as the sole carbon and energy source. An optimization framework merging global, single-objective, multi-objective, and Bayesian methods was developed and applied to these datasets to quantify the predictive and parameter uncertainty associated with each model. A combination of Bayes information criteria as well as a Bayesian approach to hypothesis testing and parameter correlation allowed for an objective approach to model selection, model predictive accuracy quantification, and an assessment of the strength of dependencies between calibrated parameters. Finally, a variance-based approach to global sensitivity, explicitly accounting for dependencies between estimated parameters, was employed to assess the influence of model parameters on model predictions describing cellular growth and MC metabolism.

2. Materials and methods

A roadmap is presented to first illustrate the workflow of the Materials and Methods section (Fig. 1). First (Section 2.1), we present a brief overview of the unstructured kinetic modelling framework as well as a complete description of the experimental data collection effort. Section 2.2 introduces the primary components of the model-data fitting approach, which is thoroughly detailed in a companion paper (Manheim and Detwiler, 2018). Bayes information criteria, that were used to objectively compare and select the appropriate model describing MC biodegradation, are reviewed in Section 2.3. Furthermore, the Bayesian approach to hypothesis testing and correlation analysis, which quantified differences in model predictive accuracy and the strength of dependencies between calibrated parameters, is presented in Section 2.4. Lastly, the variance-based approach to global sensitivity analysis (GSA), quantifying the influence of input parameters on the model output variance, is introduced in Section 2.5.

2.1. Summary of selected unstructured kinetic models and data collection effort

A total of eight unstructured kinetic models were reviewed in this study to predict MC biodegradation. The main assumption of these unstructured kinetic models is that bacterial growth is limited by a single substrate (i.e., MC). Coupled substrate depletion and bacterial growth kinetics for these models are described by two ordinary differential equations (ODEs) (Eqs. (1) and (2)), where the endogenous decay of bacterial cells during growth is explicitly considered (Rittmann et al., 2002; van Bodegom, 2007):

$$\frac{dS}{dt} = -\frac{1}{Y}\mu X \tag{1}$$

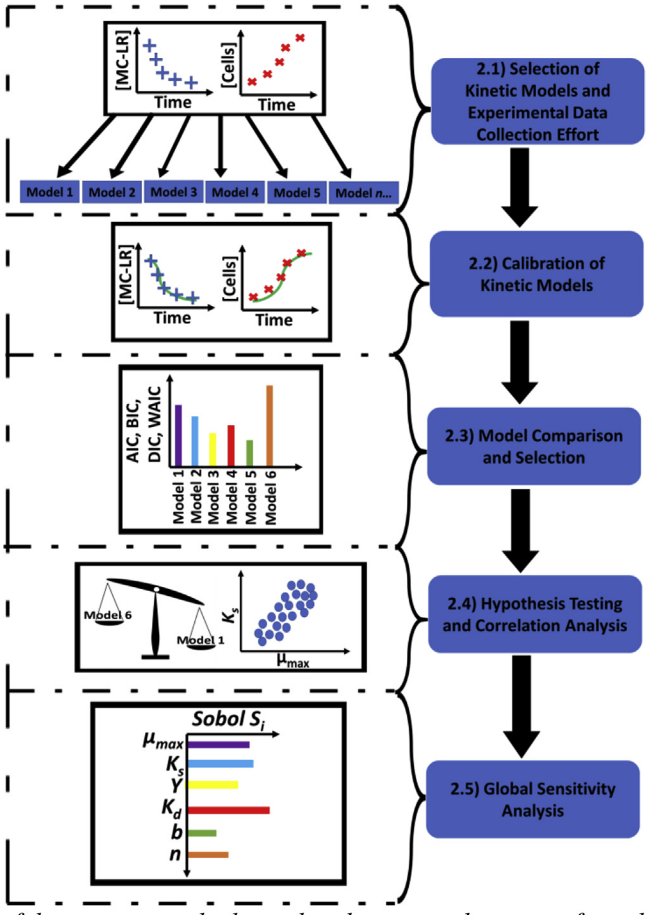

Fig. 1. A roadmap of the primary methods used in this research starting from the model selection and experimental data collection effort (Section 2.1) to the calibration (Section 2.2), model comparison and selection methods (Section 2.3), moving to the Bayesian hypothesis testing (Section 2.4), and ending in a GSA (Section 2.5).

$$\frac{dX}{dt} = \mu X - k_d X \tag{2}$$

Where S is the limiting substrate concentration (mg/L), X is the biomass concentration (mg/L), μ is the specific growth rate of bacterial cells (1/hr), Y is the cell yield coefficient (unitless), and k_d is the endogenous decay coefficient (1/hr). Importantly, $X = b^*C$, where b is a linear scaling factor used to convert optical density or cell concentration data (C) into biomass concentrations (X).

Table 1 contrasts the unstructured kinetic models surveyed in this study to define the nonlinear relationship between limiting substrate concentration (S) and specific growth rate (μ). Here, we briefly compare the differences in mathematical structure and mechanisms accounted for by each model:

- The classical model of Monod, (1949), analogous to the Michaelis Menten enzyme kinetic model, defines the specific growth rate (μ) as a hyperbolic function of substrate concentration (S) with three main parameters: the maximum specific growth rate, half saturation constant, and the yield coefficient (μ_{max}, K_s, and Y) (Table 1);
- The Tessier model (Tessier, 1942) describes the specific growth rate as an exponential function of the substrate concentration, μ_{max}, and K_s (Table 1);
- The Contois model (Contois, 1959) accounts for changes in population density that affect the net specific growth rate through inclusion of the biomass concentration, X, into the existing Monod framework (Table 1);
- The Blackman model (Blackman, 1905) defines a first-order relationship between specific growth rate (μ) and substrate concentration at low substrate concentrations and a zero-order relationship at higher substrate concentrations (above a threshold concentration, 2^*K_s) (Table 1);
- The Moser (1958) model accounts for potential interactions between binding sites on the enzyme molecule by integrating a tunable parameter n into the Monod framework (analogous to Hill's enzyme kinetic equation, Panikov and Pirt, 1978).
- Powell (1967) considered the effect of passive diffusion of a given substrate as the main rate limiting step affecting bacterial growth, deriving the equation in Table 1;
- Dabes et al. (1973) derived a "three-parameter" model describing bacterial growth on a single limiting substrate by considering that only two of the long series of catalyzed, reversible enzyme-substrate reactions involved in substrate metabolism had slow reaction rates (Table 1);
- By simplifying cellular processes to a coupled system of anabolic and catabolic reactions, Heijnen and Romein (1995) developed a universal microbial growth and substrate uptake model (Table 1).

Experimental data were obtained from four studies quantifying MC biodegradation kinetics of isolated bacterial populations (Table 2) (Valeria et al., 2006; Wang et al., 2010; Xiao et al., 2011; Zhang et al., 2015). These studies isolated bacterial populations from the *Sphingomonas*, *Sphingopyxis*, and *Bacillus* genera, which are representative of the main populations involved in MC degradation via the well-known *mlr* pathway (Bourne et al., 1996, 2001; Li et al., 2017). The few studies that cultured isolated bacteria using MC as the sole carbon and energy source were selected because they agreed with the main model assumption described above.

Each study performed batch degradation experiments, where the initial bacterial inoculum and MC concentrations were controlled (200 μg/L-42 mg/L) (Table 2). These studies promoted aerobic biodegradation of MC (i.e., through shaking) and were temperature controlled (23–30 °C) (Table 2). Very few studies were observed in the literature that reported bacterial growth in conjunction with MC degradation, where those that did only reported optical density (Wang et al., 2010; Xiao et al., 2011; Zhang et al., 2015) or cell count measurements (Valeria et al., 2006). As the units of cell concentration in Equation (2) are defined in mass per volume (mg/L), optical density and cell concentration measurements were converted to cell biomass concentrations during model fitting.

2.2. Model-data fitting approach

Bivariate experimental datasets subject to model calibration in this study described time varying concentrations in MC and biomass. Both the sparse and noisy data as well as the highly nonlinear nature of the models presented a complex optimization problem (Manheim and Detwiler, 2018). We applied a combination of single objective (SO) global optimization, multi-objective (MO) global optimization, and strictly Bayesian based evolutionary algorithms to determine an accurate and defined range in model parameters (Fig. 2, refer to Manheim and Detwiler, 2018).

A SO algorithm (AMALGAM-SO, Vrugt et al., 2009) was first applied to ascertain the location of the global minimum and the best fits for extremely biased solutions (i.e., fitting one variable and not the other). An MO optimization approach (using the NSGA-III

Table 1
Summary of unstructured kinetic models implemented in this study.

Model #	Reference	Model Structure	Main Parameters
1	Monod (1949)	$\mu = \frac{\mu_{max} S}{K_s + S}$	μ_{max}, K_s
2	Tessier (1942)	$\mu = \mu_{max}\left[1 - \exp\left(\frac{-S}{K_s}\right)\right]$	μ_{max}, K_s
3	Contois (1959)	$\mu = \frac{\mu_{max} S}{K_s X + S}$	μ_{max}, K_s
4	Blackman (1905)	$\mu = \mu_{max}$ if $S \geq 2Ks$ $\mu = \frac{\mu_{max}}{2K_s} S$ if $S < 2Ks$	μ_{max}, K_s
5	Dabes et al. (1973)	$\mu = \mu_{max} \frac{1 + \frac{S}{K_s} + \propto}{4\propto}\left[1 - \left\{1 - \frac{8\propto \frac{S}{K_s}}{\left(1 + \frac{S}{K_s} + \propto\right)^2}\right\}^{1/2}\right]$	$\mu_{max}, K_s, \propto$
6	Powell (1967)	$\mu = \mu_{max} \frac{1 + \frac{S}{K_s} + \propto}{2\propto}\left[1 - \left\{1 - \frac{4\propto \frac{S}{K_s}}{\left(1 + \frac{S}{K_s} + \propto\right)^2}\right\}^{1/2}\right]$	$\mu_{max}, K_s, \propto$
7	Moser (1958)	$\mu = \frac{\mu_{max} S^n}{K_s + S^n}$	μ_{max}, K_s, n
8	Heijnen and Romein (1995)	$\mu = \mu_{max}\left[\frac{\frac{S}{K_s}}{\frac{S}{K_s} - 1 + 2^{1/n}}\right]^n$	μ_{max}, K_s, n

algorithm) was applied to both confirm the SO results and to define an optimal region in the search space where the corresponding solutions were unbiased (i.e., the "compromise" solution space) (Wohling et al., 2008; Deb and Jain, 2014) (Fig. 2). Finally, an Approximate Bayesian Computation (ABC) approach (using the DREAM-ZS algorithm, Laloy and Vrugt, 2012) was adopted to quantify the uncertainty associated with the parameter estimates and the model predictions (Sadegh and Vrugt, 2014) (Fig. 2). Optimization results using this method are summarized in a supplementary dataset for reference (see Supplementary Material). In addition, a range in model parameters (i.e., μ_{max}, K_s, Y) was compiled from relevant biodegradation literature to confine the search space to a realistic range in values (Supplementary Information, section 1).

2.3. Bayesian model comparisons and selection

A Bayesian framework for model predictive accuracy was applied to compare and select the best performing models (Gelman et al., 2014). Two popular approaches have been detailed in Gelman et al. (2014) and Christensen et al. (2011). The first approach calculates several information criteria (i.e., AIC, BIC, DIC, WAIC, which are defined in Section 2 of the Supplementary Information) that have been developed to assess model predictive accuracy. Smaller

Table 2
Summary of experimental conditions in each study selected.

Study #	Reference	Taxonomic Identity	Culture Conditions	MC Variant (Media)	Initial MC Conc. (mg/L)	Initial Bacterium Conc.
1	Zhang et al. (2015)	*Bacillus nanhaiencis* strain JZ-2013	Batch growth, shaken at 30 °C	LR (M9)	15	OD (600 nm) ~0.514
2	Wang et al. (2010)	*Sphingopyxis* sp. USTB-05	Batch growth, shaken at 200 rpm, 30 °C	RR (Modified MSM)	42.3	OD (600 nm) ~0.004
3	Valeria et al. (2006)	*Sphingomonas* sp. CBA4	Batch growth, shaken at 23 ± 2 °C	RR (MSM)	0.200	1.20E06 CFU/mL
4	Xiao et al. (2011)	*Sphingopyxis* sp. USTB-05	Batch growth, shaken at 200 rpm, 30 °C	LR (Modified MSM)	28.8	OD (600 nm) ~0.019

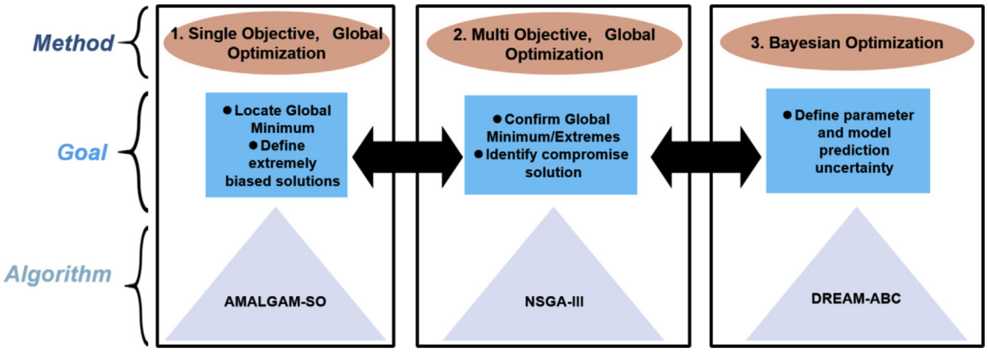

Fig. 2. The primary optimization methods, goals, and algorithms used in this study for parameter estimation.

values of each information criterion indicate better model performance. The second approach is to define the log pseudo marginal likelihood (LPML) of selecting a certain model given the data (Geisser and Eddy, 1979). Higher values of the LPML criterion indicate better model performance. Details concerning the calculations involved, an overview of the ranking method, and summary of the results are presented in Section 2 of the Supplementary Information.

2.4. *Bayesian significance testing and correlation analysis*

A quantitative framework for Bayesian hypothesis testing, termed Bayesian Estimation Supersedes the T-test (BEST) was adopted in this study to compare the predictive accuracy of the best and next best performing models (Kruschke 2011, 2013). Using the BEST framework, we tested the hypothesis that the predictive accuracy of both models was equivalent. The BEST method relies on a Bayesian approach to fit a t-probability distribution to the distribution in log-likelihoods obtained from the calibration procedure of both models (using the DREAM-ZS algorithm, Supplementary Information, section 3). Next, three probability distributions are derived from the difference in posterior distributions of central tendencies (means), variabilities (standard deviations), and effect sizes (see Supplementary Information, section 3). The effect size is a statistical parameter used to quantify the size of the difference between two different populations and is calculated using a combination of the means/standard deviations between both distributions $\left(\frac{\mu_1 - \mu_2}{\sqrt{\frac{\sigma1^2 + \sigma2^2}{2}}}\right)$ (Coe, 2002). Based on the degree of overlap between the distribution in each of these differences (using a 95% highest density interval) with a defined region of practical equivalence (ROPE, −0.1 to 0.1 for all distributions) around the null value (0), the initial hypothesis can be accepted or rejected (Kruschke 2011, 2013).

The correlation among different model input parameters was assessed using a Bayesian counterpart to Pearson's linear correlation model. A bivariate normal distribution was used as the main model framework to estimate several probability distributions in Pearson's correlation coefficient (ρ) between different model input parameters. The DREAM-ZS algorithm was used to fit the bivariate distribution model to the posterior distributions in model parameters achieved from the optimization procedure (using two parameter values at a time) (Supplementary Information, section 4).

2.5. *Global sensitivity analysis (GSA)*

GSA has progressed into one of the most powerful and robust approaches to investigate the influence of different model input parameters on output predictions (Saltelli et al., 2008; Razavi and Gupta 2015, 2016a; 2016b; Gupta and Razavi, 2017). GSA investigates the model response when varying each input parameter across its entire uncertainty range, thereby allowing a comprehensive outlook on parameter sensitivity (see Saltelli et al., 2008 for more complete details).

A variance based global sensitivity analysis (VBGSA) accounting for dependent model input parameters was applied in this study to analyze the effects of different model input parameters on predicted responses (Mara et al., 2015). This method allows the GSA to be conducted unobstructed from the correlations that may be present between input parameters, allowing unique sensitivity indices to be derived. Sobol's first and total order effect indices can be reliably calculated to rank the influence of different model parameters on resulting predictions. The “first” order effect index (S_i) represents the independent contribution of an individual parameter to the total model output variance, while the “total” order effect index (ST_i) denotes the combined interactive contributions of an individual parameter with all other parameters to the total model output variance (Saltelli et al., 2008). The specifications and calculations of the sensitivity estimation procedure are summarized in the Supplementary Information (section 5).

3. Results

3.1. *Bayesian model comparison and selection*

The top three best performing models, based on a ranking system using all summarized criteria (AIC-LPML), varied across each study (Fig. 3, Tables S4–S7). The results highlighted the consistent and accurate performance of the Moser model for three of the four datasets investigated, as the AIC-WAIC criteria and LPML values were consistently lowest and highest for this model (Fig. 3, Tables S4–S7). Results for Study 4 indicated the only exception to this trend, where the Heijnen model performed the best (i.e., lowest DIC-WAIC and highest LPML, Fig. 3). The Contois model performed reasonably well for Studies 1 and 2 (lower AIC-WAIC and higher LPML), and the performance of the Blackman kinetic model was worth considering based on results presented for Studies 3 and 4 (i.e., lower overall AIC-WAIC and higher LPML, Fig. 3). However, the Monod model demonstrated poor predictive performance across all studies (i.e., higher overall AIC-WAIC and lower LPML Fig. 3, Tables S4–S7).

The quantitative strength of evidence in favor of the Moser or Heijnen models for predicting MC biodegradation was assessed using the BEST approach (Kruschke 2011, 2013). Through Bayesian fitting of a t-distribution to the log likelihood values obtained from the initial calibration procedure, a posterior distribution in means and standard deviations was reached for both competing models. The difference in this posterior distribution of means (μ_1 - μ_2), standard deviations (σ_1 - σ_2), and effect sizes $\left(\frac{\mu_1 - \mu_2}{\sqrt{\frac{\sigma1^2 + \sigma2^2}{2}}}\right)$ between the best and next best performing model provides quantitative evidence of the magnitude of the difference in predictive accuracies between the competing models.

Fig. 4 details the probability densities of the difference in means, standard deviations, and effect sizes between the best and next best performing models for each study. For Studies 1–4, the best and second-best performing models were as follows: Moser and Contois; Moser and Contois; Moser and Heijnen; as well as Heijnen and Moser. The results demonstrated that the predictive accuracies of the best and next best performing model were significantly different for each study, which is supported by the following evidence: 1) the distributions of the difference in means and standard deviations between the competing models were centered well away from zero; 2) the 95% highest density intervals (HDI) of the differences in means/standard deviations did not overlap the “null value” (0); 3) the magnitude of the differences in effect size was large; and 4) the 95% HDI of the effect sizes were well outside the range of the ROPE [-0.1, 0.1] interval (Fig. 4, McGraw and Wong, 1992; Kruschke, 2011; Kruschke, 2013). These results confirm that: 1) there is statistically significant evidence in favor of the Moser or Heijnen models and 2) that model selection (and associated growth mechanisms included) greatly influences predictive performance of MC biodegradation.

3.2. *Model-data fits and parameter distributions*

Both the Moser (Studies 1–3) and Heijnen (Study 4) models were able to accurately reproduce MC biodegradation and biomass

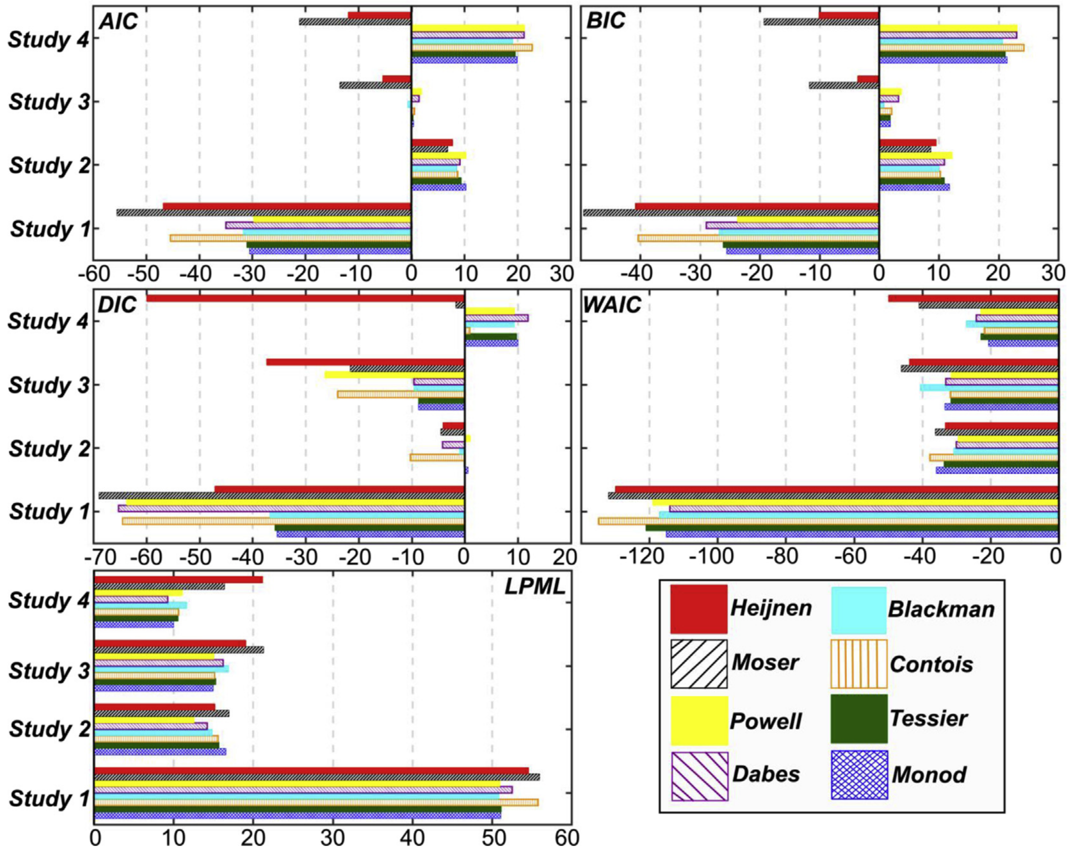

Fig. 3. Comparison of unstructured kinetic model predictive accuracy using Bayesian information criteria (AIC-WAIC) and Log Pseudo Marginal Likelihood (LPML) values calculated for each study and model. Lower values of AIC, BIC, DIC, and WAIC or higher values of LPML are associated with improved model predictive accuracy. According to all AIC/BIC, and LPML as well as most DIC/WAIC calculations, the Moser and Heijnen model predictions outperform all other models for Studies 1–3 and 4, respectively.

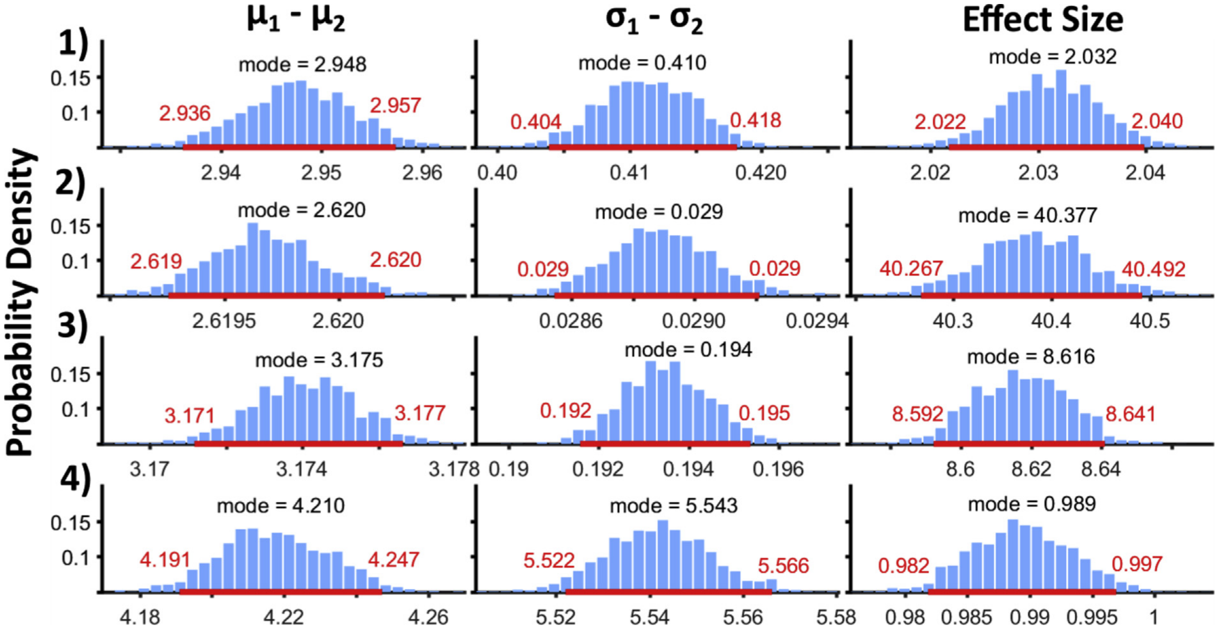

Fig. 4. Statistical differences in densities of model predictive accuracies (log likelihoods) associated with the best performing vs. the next best performing kinetic models for Studies 1–4. Using the BEST approach, the distribution in predictive accuracies (log-likelihoods) for the best and next best performing models is fitted to a t-distribution, returning a posterior distribution in means, standard deviations, and effect sizes. The difference in the posterior distributions of fitted means (column "μ_1-μ_2"), standard deviations (column "σ_1-σ_2"), and effect sizes (column "Effect Size") between the best and next best performing model forms a final distribution that determines the quantitative strength of evidence in favor of the best performing model. Both the 95% highest density intervals (in red) and the modes (black) of each final distribution are indicated on each figure. (For interpretation of the references to color in this figure legend, the reader is referred to the Web version of this article.)

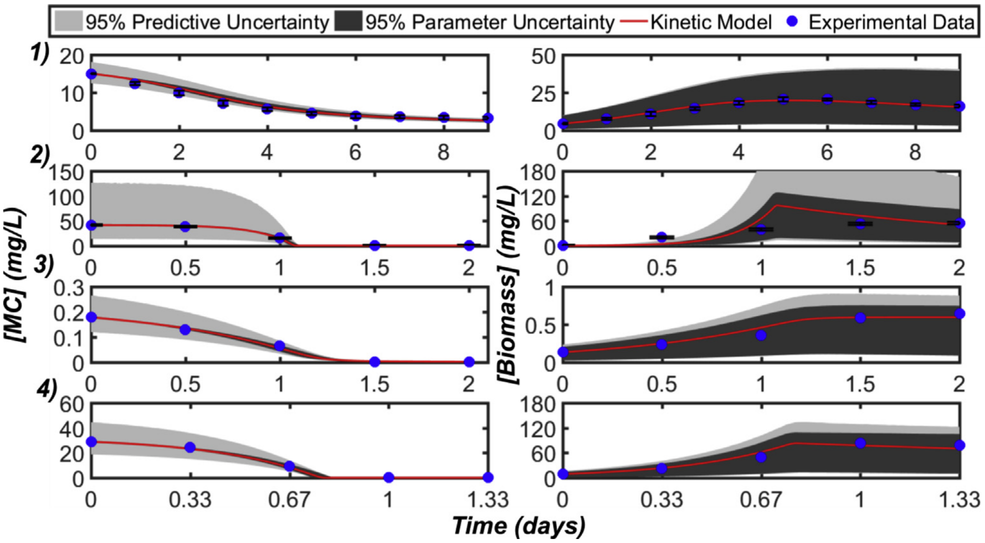

Fig. 5. Kinetic model-experimental data fitting results of the best performing model for Studies 1–4 portraying MC removal (first column) and corresponding biomass growth (second column). Studies 1–3 were fit using the Moser model, whereas Study 4 was fit using the Heijnen model. The red line indicates the best fitting model prediction, while the blue dots represent the experimental data points (along with the standard deviation of replicate experiments). The light grey shading indicates the 95% predictive uncertainty interval and the dark grey shading represents the 95% uncertainty interval associated with the parameter estimation. Narrower total and parameter uncertainty intervals are indicative of improved model predictive accuracy. All experimental data points were observed to fall within the uncertainty intervals, indicating that the predictions afforded by either model can reproduce the experimental data with great certainty. (For interpretation of the references to color in this figure legend, the reader is referred to the Web version of this article.)

growth for each of the four studies reviewed, as the experimental data fell within the 95% total predictive uncertainty intervals (Fig. 5). The accuracy of, and certainty in, model predictions were highest for Study 1 (*Bacillus nanhaiencis* strain) and lowest for Study 2 (*Sphingopyxis* sp. strain), as noted by the width of the uncertainty intervals, the proximity of the best fitting prediction to the experimental data, as well as the RMSE and minimum objective function values (Fig. 5, Table S8).

Parameter uncertainty was in all cases higher for the biomass growth data as compared to the substrate consumption data, as demonstrated by the wide 95% uncertainty intervals (Fig. 5). This result can be explained by both the high parameter uncertainty associated with the yield coefficient (Y) and endogenous decay rate (k_d) parameters (Table 3) and moderate to high sensitivity of the predicted cell concentrations to these model parameters (Fig. 8). When an input parameter to a given model is both highly uncertain and influential, the total predictive uncertainty of this model will be higher, resulting in a wide range of predictions in biomass growth (Fig. 5).

The posterior distributions in best performing model parameters were fairly normally distributed for μ_{max}, k_d, b, and n model parameters, indicating that they were well identified during model-data calibration (Fig. 6). This result was further supported by the small 95% credible interval widths and COV values obtained for these model parameters (Table 3). The half-saturation constant (K_s) could not be uniquely identified for Studies 1 and 4; however, K_s was well distinguishable given the experimental data from Studies 2 and 3 (supported by the small 95% credible intervals and COVs), although the distributions were very right-skewed (Fig. 6). The yield coefficient values (Y) could not be uniquely identified for all studies investigated, as all parameter values approached the upper realistic boundary (Fig. 6). The best performing parameter values were present close to the peak of each posterior distribution, further verifying that the distributions converged around the best compromise solution (Fig. 6).

Diverse kinetic and physical growth characteristics were evidenced for each MC degrading bacterium included in this study, especially when comparing maximum specific growth rate and half-saturation constant model parameters (Table 3). Maximum specific growth rates on MC were not necessarily proportional to MC affinities (i.e., K_s). For example, the *Sphingopyxis* sp. *USTB-05* (Study 2) strain was characterized by a relatively low affinity for MC (moderate-high K_s), but had the highest maximum specific growth rate of the studies investigated. Comparably, the *Sphingomonas* sp. evidenced a very high affinity for MC as a substrate but had the lowest maximum specific growth rate of the studies investigated (Table 3). Great differences in the magnitude of conversion constants (b) implicated highly varying cell densities and physiologies for each MC degrading bacterium. Across all studies, the magnitude of the yield coefficient (Y), endogenous decay rate (k_d), and n values were relatively comparable (Table 3).

3.3. Parameter correlation analysis

The parameter correlation analysis indicated that for all studies (1–4), there was a strong, positive, linear correlation between μ_{max} and k_d as well as between b and Y model parameters (Fig. 7), where distributions in Pearson's correlation coefficient varied between 0.53 and 0.92 (for μ_{max} and k_d) as well as between 0.80 and 0.90 (b and Y). Study 1 demonstrated a strong, negative, and non-linear correlation between μ_{max} and n model parameters. Studies 2–4 indicated a moderate, negative, and linear correlation between μ_{max} and b model parameters. Studies 2–3 observed a strong, negative, and slightly non-linear correlation between n and K_s values (Fig. 7). Across all studies, the mostly negative correlations between parameters n and K_s/μ_{max} were non-linear given that the n value parameters were used as exponents in the original model structures (for Moser and Heijnen). The presence of multiple strong positive and negative linear and nonlinear correlations was a factor that likely prohibited the unique identification of all six model parameters given the experimental data from all studies.

Table 3
Summary of best performing model parameter values including the mean (μ), standard deviation (σ), coefficient of variation (COV), and 95% credible intervals.

Parameter	μ_{max} (1/day)			
Study	1	2	3	4
μ	1.48	6.11	1.43	3.31
σ	0.799	0.290	0.177	0.392
COV	54	5	12	12
95% Credible Interval	[0.659, 3.80]	[5.53, 6.59]	[1.11,1.78]	[2.64,4.02]
Parameter	**K_s (mg/L)**			
Study	1	2	3	4
μ	188	3.93	0.000194	30.1
σ	26.2	3.52	9.37E-05	47.4
COV	14	90	48	157
95% Credible Interval	[127, 219]	[0.159,12.3]	[0.00010,0.00043]	[1.54,196]
Parameter	**Y (mg biomass/mg substrate)**			
Study	1	2	3	4
μ	2.43	2.42	2.47	2.36
σ	0.859	0.860	0.836	0.906
COV	35	36	34	38
95% Credible Interval	[0.525, 3.48]	[0.536,3.48]	[0.588,3.48]	[0.433,3.48]
Parameter	**k_d (1/day)**			
Study	1	2	3	4
μ	0.140	0.739	0.172	0.406
σ	0.0584	0.1908	0.1191	0.258
COV	42	26	69	64
95% Credible Interval	[0.0318, 0.245]	[0.329,0.991]	[0.014,0.450]	[0.0278,0.925]
Parameter	**b ((g DW/L)/OD or (g DW/L)/(CFU/mL))**			
Study	1	2	3	4
μ	0.0094	0.0620	9.6E-11	0.389
σ	0.0044	0.0257	3.85E-11	0.176
COV	47	41	40	45
95% Credible Interval	[0.00173, 0.0191]	[0.012,0.109]	[2.01E-11, 1.72E-10]	[0.0621,0.751]
Parameter	**n (unitless)**			
Study	1	2	3	4
μ	2.00	6.82	2.17	1.96
σ	0.289	1.573	0.090	0.042
COV	14	23	4	2
95% Credible Interval	[1.49, 2.57]	[4.37,9.73]	[1.98, 2.31]	[1.84, 2.00]

3.4. Global sensitivity analysis

The results of the VBGSA indicated a diverse range in input parameter sensitivities across all studies using Sobol's first and total order effect indices as the primary means of comparison (Fig. 8). It is important to note that Sobol's first order effect indices closer to 1 indicated that the model output was more sensitive to the corresponding input parameter, whereas indices closer to 0 indicated little to no sensitivity. Comparably, values of Sobol's total order effect index closer to or higher than 1 were indicative of a parameter that was highly interacting with other model parameters (and not interacting when values approached 0).

Based on a unique ranking system (described in S.I., section 5.3, the general parameter rankings across studies (using either first- or total-effect indices), from most to least influential, depended primarily on the variable of interest (i.e., substrate or cell biomass concentrations) (Fig. 8). Using the first-order indices (S_i) as ranking criteria, predicted substrate concentrations were generally most influenced (in descending order) by k_d (1), b (2), and μ_{max} (3), with less influence observed from Y (4), K_s (5), and n (6) (Fig. 8I). Predicted cell biomass concentrations were most influenced (in descending order) by parameter values of k_d (1), μ_{max} (2), and K_s (3), with less influence observed from Y (4), b (5), and n (6) (Fig. 8II). Using the total order effect indices (ST_i) as ranking criteria, interactive effects on substrate concentration predictions were higher for k_d (1), K_s (2), Y (3) and less significant for n (4), μ_{max} (5), and b (6) model parameters (Fig. 8I). Comparably, interactive effects on cell biomass concentration predictions were higher for k_d (1), μ_{max} (2), K_s (3) and less significant for Y (4), b (5), and n (6) model parameters (Fig. 8II).

4. Discussion

4.1. Study contribution

This is the first study, to the best of our knowledge, to apply and compare several unstructured kinetic growth models to describe MC biodegradation. Coupled bacterial growth and MC removal kinetics were both accounted for in all unstructured models, which is a significant step forward from previous simplistic zero- and first-order kinetic models to describe MC biodegradation. Each unstructured model was successfully calibrated to existing experimental data through a novel optimization approach to determine an accurate and defined range in bio-kinetic parameters. These parameters can eventually, through further refinement, model complexity, and experimentation, be applied to the design of biological water treatment systems and prediction of the fate and persistence of MC in the environment.

The results from this study represent a preliminary step toward the development of a practical and comprehensive unstructured kinetic model that can predict the environmental behavior of these microorganisms. Clearly, accounting for different environmental

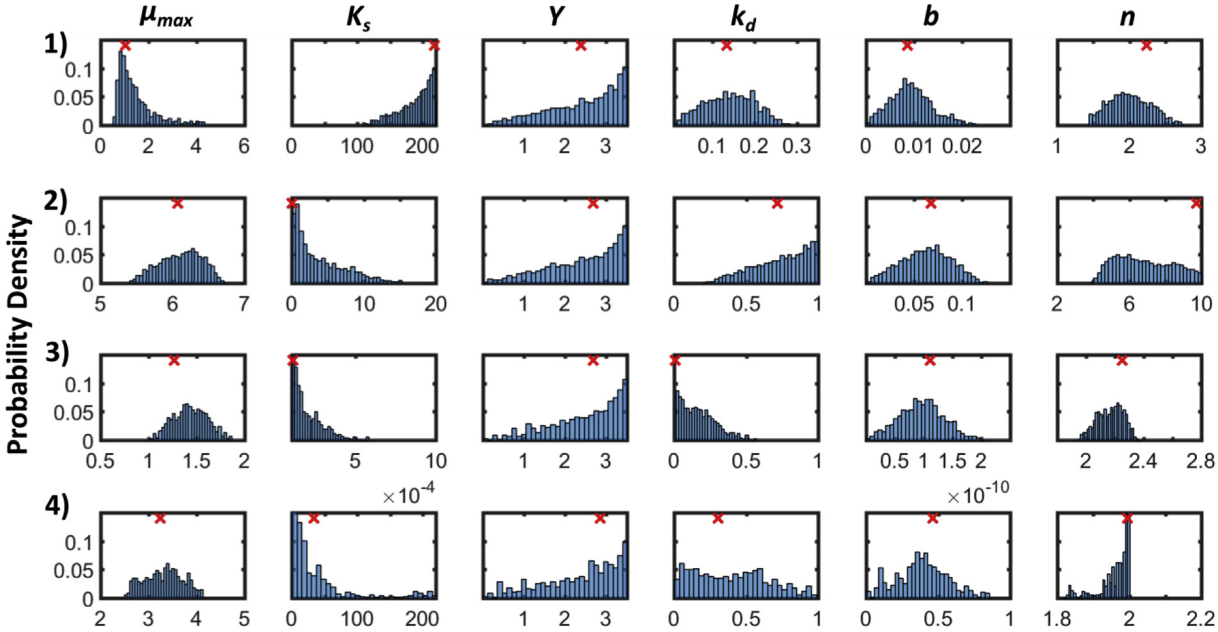

Fig. 6. Posterior distributions in best performing model parameters for Studies 1–4 obtained from the DREAMZS_ABC algorithm. Studies 1–3 were fit using the Moser model, whereas Study 4 was fit using the Heijnen model structure. Distributions that appear normally distributed indicate uniquely identifiable parameters, whereas flat or left/right skewed distributions indicate issues with unique identification (and possible correlation with other parameters). The red 'x' indicates the best fitting model parameter (MAP) value for each study. In most cases, the MAP falls on the location with the highest probability density. (For interpretation of the references to color in this figure legend, the reader is referred to the Web version of this article.)

factors in the model structure, such as temperature, pH, or the presence of other carbon substrates (as discussed in Section 4.5) will better capture the environmental variability expected in practice. As the complexity of these models is expected to increase in future studies to account for various environmental factors, we argue that issues associated with model selection, uncertainty estimation, nonlinear regression, and parameter identification will likely intensify. The approach presented herein for model selection and calibration provides a robust foundation for developing MC biodegradation models for increasingly complex environmental conditions.

4.2. The physical case for Moser kinetics

The statistical results presented in this study have demonstrated that the Moser model provided superior MC biodegradation predictions compared to other common unstructured kinetic models. However, we have not emphasized the physical relevance underpinning the structure of the Moser model. As initially proposed by Blackman (1905), many studies have advocated that the Monod model is a theoretical extension of the "bottleneck concept," postulating that a single rate limiting "master" reaction controls the kinetics of metabolism of any substrate (Monod, 1949; Dabes et al., 1973; Panikov, 1995). In the simplified case of Monod kinetics, the maximum forward rate of one reaction in the cell is order of magnitudes smaller than the maximum forward rate of any other enzyme catalyzed reactions involved in transport and/or metabolism. This concept simplifies the description of bacterial growth into a Michaelis Menten (or Hill) type rate equation, depending on one enzyme and reaction of interest (Dabes et al., 1973; Panikov, 1995).

We have shown statistically that accounting for the mechanisms of saturation, binding affinity, and binding interactions between this hypothetical enzyme and MC substrate complex can accurately and reliably predict MC biodegradation. A "master" rate-limiting reaction dictating MC biodegradation kinetics is further supported by the fact that the model comparison process did not select for a more complex, multiple reaction type derivation as provided by Dabes et al. (1973). Importantly, the mechanism of "saturation" involves binding of substrate molecules to the active sites on the enzyme to capacity; "binding affinity", the relative strength of attraction or attachment between an enzyme and substrate molecule; and "interactions", the degree of inhibition or facilitation between binding sites on a given enzyme (Panikov and Pirt, 1978; Cohlberg, 1979; Panikov, 1995).

Given this theoretical justification to the Moser model, it is interesting to explore which "master" reaction may be the most well justified rate limiting step in the MC biodegradation pathway. MC biodegradation involves four primary genes/enzymes, including *mlr*A, *mlr*B, *mlr*C, and *mlr*D (production of the enzyme microcystinase (*Mlr*A), enzyme *Mlr*B, enzyme *Mlr*C, and enzyme *Mlr*D) (Bourne et al., 1996, 2001). *mlr*A is responsible for the initial linearization of cyclical MC, *mlr*B and *mlr*C for further breaking down linearized MC into smaller peptide and amino acid products, and *mlr*D for actively transporting MC into the cell (Bourne et al., 1996, 2001).

It is probable that the linearization of cyclical MC may be the rate limiting step in this pathway, given that the cyclical structure is highly resistant to degradation and may require a large cellular energy input to synthesize adequate quantities of microcystinase (Dziga et al., 2012). Experimental evidence of the enzymatic activity of microcystinase has indicated that Hill kinetics best describe the linearization reaction as compared to Michaelis-Menten enzyme kinetics. Dziga et al. (2012) results align with the statistical results observed from this study, which advocated the Moser model over the Monod model. In addition, the kinetic parameters measured for microcystinase ($V_{max} = 95$ day^{-1}, $Ks = 158$ mg/L, $n = 1.57$) were on the same order of magnitude of those observed for various MC degrading bacteria in this study, further strengthening our initial presumption.

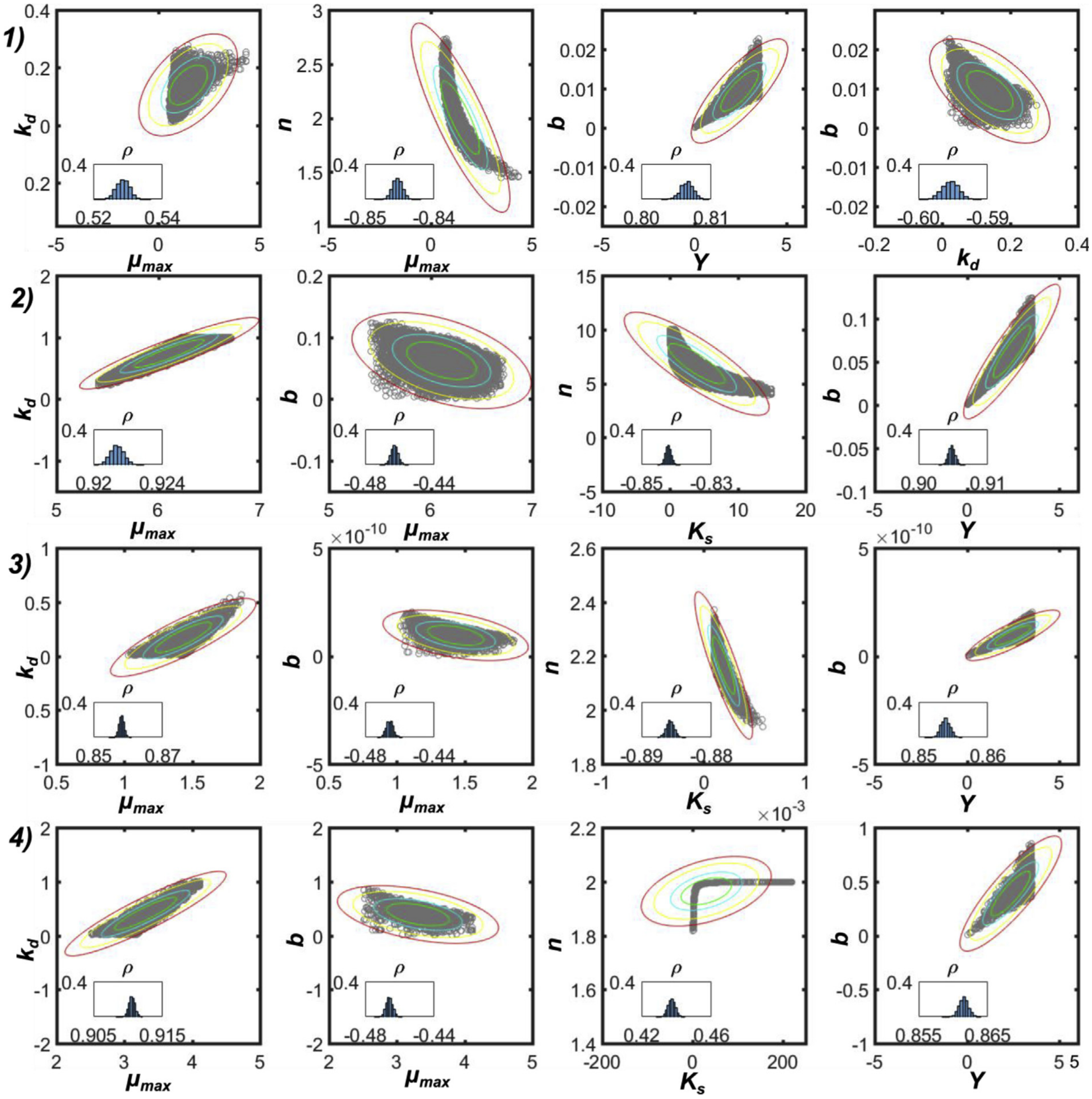

Fig. 7. Bayesian analysis of the strongest (i.e., $\rho > 0.40$, $\rho < -0.40$) linear correlations between best performing model parameters for Studies 1–4. The 99%, 95%, 75%, and 50% highest density ellipses are overlaid on the scatter plots in red, yellow, cyan, and green, respectively. The inlet plots depict the distribution in Pearson's correlation coefficient obtained from the Bayesian correlation analysis. Although the pairwise combinations of strongest linear correlations were not always equivalent across all studies, strong positive correlations (higher values of Pearson's ρ) were generally evidenced for μ_{max} vs. k_d and Y vs. b, whereas negative correlations were generally observed for μ_{max} vs. b. Some nonlinearity in the correlations were also evidenced for model parameters that involved exponents in the original model structure (i.e., n). (For interpretation of the references to color in this figure legend, the reader is referred to the Web version of this article.)

4.3. Physical significance of model parameter estimates

The physical significance of the Moser model parameters is also important to review. The results demonstrated that all MC degrading bacteria possessed similar ranges in maximum specific growth rates (1–7 per day), which are comparable to the lower range in maximum specific growth rates reported for fast growing, heterotrophic microorganisms in activated sludge systems (Kovárová-Kovar and Egli, 1998; Tchobanoglous et al., 2003). These results imply that these MC degrading organisms may grow relatively quickly in the environment if MC is readily available.

Very significant differences in K_s values were estimated between MC degrading bacteria in this study. Since the inverse of the half saturation constant can be defined physically as an enzyme's relative binding affinity for a substrate (Kovárová-Kovar and Egli, 1998), there are possibly marked preferences in MC as a substrate among various MC degrading bacteria. Across all MC bacteria reviewed, the *Sphingomonas* species had the lowest reported half saturation constant, which resulted in much higher specific growth rates at lower substrate concentrations. Smaller K_s values for MC substrates may signify a high specificity of microcystinase enzymes for MC as a substrate, or differences in enzyme regulation at the molecular level (i.e., induction vs. constitutive production), among many factors (Bally and Egli, 1996). A high affinity for a given substrate may be a physiological adaptation to improve an organism's capability to scavenge for several carbon sources under low

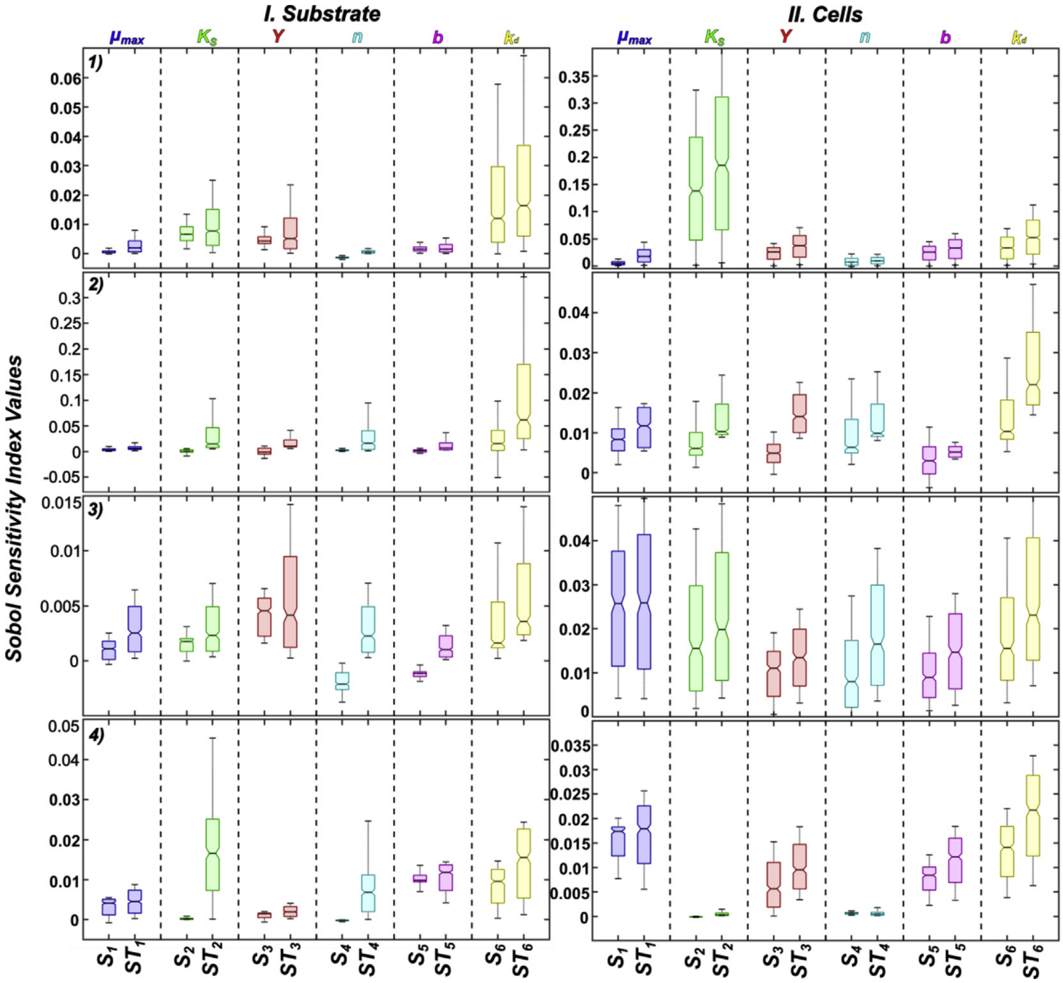

Fig. 8. VBGSA results summarized for Studies 1–4, presenting Sobol's first and total order effect indices. Here, "first" order represents the independent contribution of an individual parameter to the total model output variance, while "total" order denotes the combined interactive contributions of an individual parameter with all other parameters to the total model output variance. We note that by implementing the method of Mara et al. (2015), the sensitivity indices are determined free of any correlations present between input parameters. Values of the first order effect closer to 0 or 1 indicate that the model output is barely or highly sensitive to the corresponding input parameter, respectively. Values of the total order effect closer to 0 or 1 (or above) indicate that the parameter is hardly or highly interactive with all other model parameters, respectively. The boxplots represent the distribution in sensitivity indices across all simulated time points. Colors correspond to individual parameter values. Panel column I presents the sensitivity results for model predictions involving substrate concentration, whereas Panel column II presents results for model predictions involving cell biomass. (For interpretation of the references to color in this figure legend, the reader is referred to the Web version of this article.)

nutrient conditions present in many oligotrophic environments (Noel and Narang, 2009; Egli, 2010).

Yield coefficient (Y) parameter estimates were very high among all MC degrading bacteria. It is important to note that the yield coefficients estimated in this study are "observed" or "apparent" values, not entirely corrected for the presence of maintenance costs (Esener et al., 1983; von Bodegom, 2007). For perspective, estimated yield coefficients from the literature for the biodegradation of organic and synthetic pollutants were observed to rarely exceed 1 (i.e., 100% conversion of substrate to biomass) (Doran, 1995; Suarez and Rifai, 1999; Shuler and Kargi, 2002). Higher values of the yield coefficient estimated in this study may suggest that MC is a superior carbon source for the creation of raw cellular material as compared to the supply of the MC degrading cell's other functions.

The n parameter values for both the Moser and Heijnen models were typically greater than 1 for most studies. For the Moser model structure, this result signifies that the interactions between binding sites for MC degrading enzymes are cooperative in nature. Analogous to the Hill model for enzyme kinetics, cooperative interactions imply that the binding potential of MC substrate molecules to the enzymes involved increases as the number of previously bound substrate molecules increase (Panikov and Pirt, 1978).

The endogenous first-order decay coefficient (k_d) represents the amount of energy diverted to a cell's maintenance requirements in the absence of substrate from the environment, and usually involves oxidation of a cell's internal reserves (Rittmann et al., 2002; von Bodegom, 2007). Results from this study indicated that first order decay parameter estimates are relatively high for MC degrading populations (0.1–0.7 per day), on the same order of magnitude of those estimated for mixed bacterial populations in activated sludge (Tchobanoglous et al., 2003). These results imply that in the absence of MC or other carbonaceous substrates, a swift decline in populations may ensue in the environment.

4.4. Initial kinetic model predictions

A significant implication from initial predictions using the Moser model is that most bacterial growth rates are far from saturated in the environment if MC is used as a sole carbon and energy source (Fig. 9), as at least two of the bacterial strains

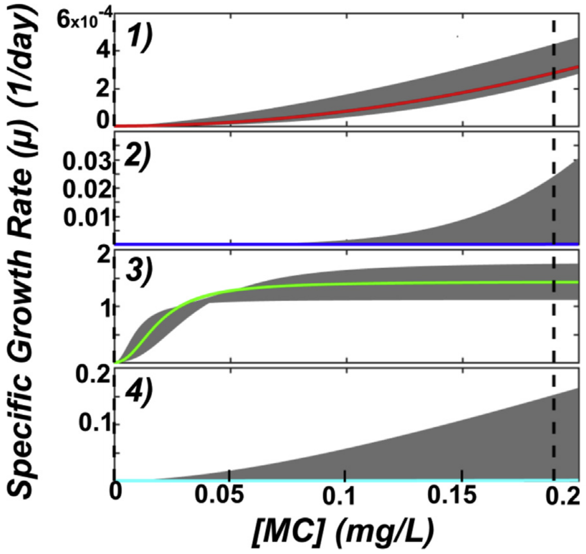

Fig. 9. Predicted specific growth rates of several MC degrading bacteria in the environment as a function of substrate concentration using the Moser (1–3) and Heijnen (4) models. The black dashed lines indicate the minimum/maximum concentrations of MC expected in the environment. The grey region and colored lines indicate the predictions associated with the lowest/highest 95% credible interval and the mean of the posterior distribution of parameter values.

(*Bacillus nanhaiencis*, *Sphingopyxis* sp. *USTB-05*) will be growing at very low specific growth rates (6E-04 to 0.2 per day). Since specific growth rate is directly proportional to substrate removal rate, we would expect slow biological removal of MC in the environment. However, when MC is supplied at much higher concentrations, as has been typically conducted in a laboratory setting (i.e., in the mg/L range), the removal rates of MC would be expected to drastically increase (1–4 orders of magnitude). Therefore, biological drinking water treatment strategies for MC removal will have to consider the disparity in specific growth rates of these organisms when faced with low concentrations of MC generally observed in the environment. A promising solution to ensure high specific growth rates of degrading bacteria and quick elimination of MC in bio-based drinking water treatment systems is through bio-stimulatory practices, like the addition of nutrients (i.e., nitrogen or phosphorus), which can perhaps maintain a stable and productive, year-round community of MC-degrading and non-degrading microorganisms (Tyagi et al., 2010; Lauderdale et al., 2012; McKie et al., 2015; Li et al., 2017).

4.5. Unstructured kinetic model limitations

Even though the unstructured kinetic models were shown to accurately characterize MC biodegradation in an ideal setting, we recognize multiple limitations to the simplifying assumptions used. First, MC may not be the primary growth limiting substrate metabolized by these degrading bacteria, since it is often present in low background concentrations (ng/L to μg/L) and not secreted until bloom senescence or collapse (Merel et al., 2013; Francy et al., 2015). In most freshwater environments, the presence of other bioavailable dissolved organic carbon represents the primary carbon and energy source for these bacteria (Egli 1995, 2010; Eleuterio and Batista, 2010). All unstructured kinetic models can be aptly modified to account for other inhibiting or stimulating substrates these bacteria may encounter in the environment (Yoon et al., 1977; Reardon et al., 2000, 2002). Future studies should consider the application of competitive multi-substrate models to better describe MC biodegradation in the environment.

Clearly, the temperature (23–30 °C) and pH (~7) employed in the batch biodegradation experiments examined in this study are ideal cases of what would be encountered in the environment. As MC degrading bacterial growth rate is highly sensitive to water temperature (25–30 °C optimal, Li et al., 2017), the predictions afforded by the current unstructured models would likely overestimate the rates of MC biodegradation in the environment. Unstructured kinetic models have been successfully tailored to account for temperature (Heitzer et al., 1991; Rosso et al., 1993; Kovárová et al., 1996), pH, or both (Rosso et al., 1995) by either considering cardinal pH and temperature properties of bacteria (mostly *E. coli* strains) or deviations of the Arrhenius equation (Alagappan and Cowan, 2004). Future studies should consider integrating these previous concepts into existing unstructured kinetic model frameworks to account for the effects of temperature and pH.

Another limiting factor to address is the fact that these unstructured kinetic models only consider the growth of isolated MC degrading populations. In the environment, these populations are part of a much more complex and interactive network of mixed microorganisms. Single organism derived unstructured model parameters are frequently applied to wastewater treatment design and engineering to characterize the behavior of complex microbial communities (Tchobanoglous et al., 2003). However, more complex mixed population models can be applied based on these single population parameter estimates and theorized interactions among certain populations, including, for example, Lotka-Volterra competition models (Faust and Raes, 2012; Song et al., 2014).

The scaling factor (b) required to convert either cell concentration or OD to biomass was identified as another limitation of the kinetic models reviewed. In this study, we assumed that there was a direct, linear relationship between OD or cell counts and dry weight biomass, which is generally the case for pure microbial cultures in practice (Kim et al., 2012; Myers et al., 2013). This assumption resulted in biomass concentrations of MC degraders ranging from 1 to 180 mg/L at stationary phase of growth. Typical dry weight biomass for activated sludge systems range from 3000 to 6000 mg/L, whereas the biomass concentrations ranged from 8 to 50 mg/L for species of bacteria degrading mixtures of BTEX compounds and PAHs (Tchobanoglous et al., 2003; Reardon et al., 2000, 2002; Knightes and Peters 2000, 2003). Thus, since the ranges in biomass predicted for this study are of similar order of magnitude to bacteria degrading petroleum hydrocarbons and far from activated sludge biomass concentrations, the use of a linear relation between OD or cell counts and biomass is well justified.

Yet another limitation of unstructured kinetic models is the assumption that the cell composition (and physiological state) remains constant during growth (i.e., "balanced growth") (Bailey and Ollis, 1976; Clark and Blanch, 1997). In the environment, growth of MC degrading organisms is expected to be "non-balanced," where cellular composition is transient with respect to fluctuations in environmental conditions (Ramkrishna et al., 1967; Fredrickson et al., 1971). Structured kinetic models can account for changes in physiological state and more comprehensively describe bacterial growth in the environment but may suffer from issues such as high complexity and computational burden (Ramkrishna et al., 1967; Fredrickson et al., 1971; Panikov, 1995).

4.6. Improving parameter identifiability: the S_0/X_0 ratio

A complete set of unique parameter estimates was not obtained for most studies. This result indicates there were more limitations in the quality of the experimental data collected, which resulted from inadequacies in the experimental design. Many studies have stressed the importance of the initial substrate to biomass (S_0/X_0) ratio when designing experiments (Dang et al., 1989; Chudoba et al., 1992; Grady et al., 1996). These studies have determined that the S_0/X_0 ratio has a drastic effect on the growth behavior and extent of physical adaptation an organism may undergo (Grady et al., 1996). In general, low S_0/X_0 ratios (<0.025 on a COD basis) were reflective of the original environmental behavior of the bacterial population ("extant" behavior), while larger S_0/X_0 ratios (>20 on a COD basis) resembled the "intrinsic" characteristics of the population under study (Dang et al., 1989; Grady et al., 1996).

Applying these criteria to our results (see Supplementary Information, section 8), the experimental conditions in Studies 1, and 3–4 resembled more "extant" behavior (S_0/X_0 ratios ranged between 1 and 3), whereas the experimental conditions for Study 2 were more "intrinsic" (S_0/X_0 were above 20). This concept helps explain why there were drastically different kinetic parameter estimates for two experiments conducted for the same species of *Sphingopyxis* degrading a different MC congener (RR vs. LR), as different S_0/X_0 ratios were used (Study 2 vs. Study 4). Maintaining this S_0/X_0 parameter at a low value is more useful for identifying parameters that will be used to predict MC removal in an environmental setting, whereas high values are more useful in an engineered setting to observe the full kinetic degradation potential of a certain MC degrading population.

The S_0/X_0 ratio also affects the parameter identifiability for a given experiment (Grady et al., 1996). Classically, there has been much controversy over how to best design a batch biodegradation experiment to obtain independent estimates of μ_{max}, K_s, and Y model parameters (Nihtilä and Virkkunen, 1977; Holmberg, 1982; Robinson and Tiedje, 1983; Liu and Zachara, 2001). For example, Robinson and Tiedje (1983) found that uncorrelated estimates of μ_{max} and K_s could be reached when performing the batch experiment in the mixed order region of the specific growth rate vs. substrate theoretical curve (at $S_0/X_0 > 20$).

Good separation of μ_{max} and K_s was observed for our results, and these parameters could be uniquely estimated for Studies 2 and 3. The experimental conditions for Studies 2 and 3 were reflective of very high S_0/X_0 ratios (Study 2–150 and Study 3–1000) (Table S9), confirming the importance of this ratio on improving parameter identifiability. However, a significant number of correlations were observed between the scaling parameter (b) and (Y) across all studies, resulting in non-unique estimates of Y. This result was concerning as the sensitivity analysis indicated that Y is an interactive and relatively influential parameter when predicting both substrate and biomass concentrations. Future MC biodegradation experiments should eliminate the use of this scaling parameter by directly measuring the biomass concentration, through dry or wet weight, protein content, or even ATP-based methods (Velten et al., 2007, 2011) to avoid unnecessary correlations developed between the scaling parameter and all other remaining parameters observed in this study.

5. Conclusions

Engineered biological treatment systems targeting the removal of MCs rely on an in-depth predictive understanding of bacterial growth. We must admit that unstructured kinetic models are not in any way comprehensive representations of the true complexity of most biological processes. However, the models reviewed in this study provided an accurate and practical approach to characterize MC biodegradation kinetics. Based on this rigorous comparison of a broad range in unstructured kinetic models, the following main conclusions were drawn from this study:

1) The underlying kinetic model structure (and associated growth mechanisms accounted for) has a statistically strong effect on model predictive accuracy and precision for MC biodegradation. In this study, the Moser model and Heijnen and Romein model were the most reliable and consistent out of all models reviewed.
2) Unique parameter estimates for MC biodegradation depend on the quality of experimental data, which is highly influenced by the experimental design (i.e., S_0/X_0 ratio). Using a new, global optimization approach, unique parameter estimates were obtained for at least three (and up to five) parameters using different experimental datasets.
3) Model predictions were generally most sensitive to the parameter values of k_d, μ_{max}, K_s, and b in the absence of correlations. Model predictions were also affected by interactions between multiple parameters. Values of k_d, μ_{max}, K_s, and Y demonstrated moderate to high levels of interactions with other parameters. These results prioritize the proper identification of k_d and Y in future studies, which were not identifiable for certain studies reviewed herein.
4) Well below saturating concentrations of MC in the environment result in minimal to no growth of MC degrading bacteria, where sub-optimal MC removal kinetics are expected in treatment practice.

We envision the results from this study as a stepping stone toward the development of a practical and comprehensive unstructured kinetic model that can reliably predict MC biodegradation in the environment. The MC-degrading bacterial populations reviewed in this study are likely underrepresented members of a more complex and dynamic community, where the clear majority of community members are less inclined to (or cannot) utilize MC as a primary carbon and energy source. However, we stress that the predictive knowledge of the isolated kinetic behavior of these bacteria metabolizing MC as a sole organic carbon source can be integrated into more complex unstructured kinetic modelling frameworks that consider multiple interacting substrates and population members as well as different environmental conditions (i.e., temperature, pH). We expect that future studies will adopt a similar model surveying and calibration approach to identify the necessary mechanisms to describe more complex environmental behavior of bacteria involved in MC biodegradation.

Conflicts of interest

The authors declare no conflict of interest.

Funding

This study was supported by the National Science Foundation, CBET under Grant No. 1806066.

Acknowledgements

We gratefully acknowledge the assistance of Dr. Thierry Mara for helping with the implementation of the variance-based sensitivity analysis for dependent parameter inputs. We also acknowledge contributions from Dr. Jasper Vrugt, who provided *MATLAB* implementations of *DREAM-ZS* and *AMALGAM-SO* optimization algorithms.

Appendix A. Supplementary data

Supplementary data to this article can be found online at https://doi.org/10.1016/j.watres.2018.11.014.

References

Alagappan, G., Cowan, R.M., 2004. Effect of temperature and dissolved oxygen on the growth kinetics of Pseudomonas putida F1 growing on benzene and toluene. Chemosphere 54, 1255–1265. https://doi.org/10.1016/j.chemosphere.2003.09.013.

Alexander, M., 1999. Biodegradation and Bioremediation, second ed. Academic Press.

Al-Khalid, T., El-Naas, M.H., 2012. Aerobic biodegradation of phenols: a comprehensive review. Crit. Rev. Environ. Sci. Technol. 42, 1631–1690. https://doi.org/10.1080/10643389.2011.569872.

Bailey, J.E., Ollis, D.F., 1976. Biochemical Engineering Fundamentals. Chemical Engineering Education.

Bally, M., Egli, T., 1996. Dynamics of substrate consumption and enzyme synthesis in *Chelatobacter heintzii* during growth in carbon-limited continuous culture with different mixtures of glucose and nitrilotriacetate. Appl. Environ. Microbiol. 62, 133–140.

Blackman, F.F., 1905. Optima and limiting factors. Ann. Bot. 19, 281–295.

Bodegom, P. van, 2007. Microbial maintenance: a critical review on its quantification. Microb. Ecol. 53, 513–523. https://doi.org/10.1007/s00248-006-9049-5.

Bourne, D.G., Jones, G.J., Blakeley, R.L., Jones, A., Negri, A.P., Riddles, P., 1996. Enzymatic pathway for the bacterial degradation of the cyanobacterial cyclic peptide toxin microcystin LR. Appl. Environ. Microbiol. 62, 4086–4094.

Bourne, D.G., Riddles, P., Jones, G.J., Smith, W., Blakeley, R.L., 2001. Characterisation of a gene cluster involved in bacterial degradation of the cyanobacterial toxin microcystin LR. Environ. Toxicol. 16, 523–534. https://doi.org/10.1002/tox.10013.

Cheung, M.Y., Liang, S., Lee, J., 2013. Toxin-producing cyanobacteria in freshwater: a review of the problems, impact on drinking water safety, and efforts for protecting public health. J. Microbiol. 51, 1–10. https://doi.org/10.1007/s12275-013-2549-3.

Christensen, R., Johnson, W., Branscum, A., Hanson, T.E., 2011. Bayesian Ideas and Data Analysis: an Introduction for Scientists and Statisticians. CRC Press, Boco Raton, FL, USA.

Chudoba, P., Capdeville, B., Chudoba, J., 1992. Explanation of biological meaning of the so/xo ratio in batch cultivation. Water Sci. Technol. 26, 743–751.

Clark, D.S., Blanch, H.W., 1997. Biochemical Engineering, second ed. CRC Press.

Coe, R., 2002. It's the Effect Size, Stupid: what effect size is and why it is important. In: Presented at the Annual Conference of the British Educational Research Association, University of Exeter, England, September 12th-14th.

Cohlberg, J.A., 1979. Km as an apparent dissociation constant. J. Chem. Educ. 56, 512. https://doi.org/10.1021/ed056p512.

Contois, D.E., 1959. Kinetics of bacterial growth: relationship between population density and specific growth rate of continuous cultures. Microbiology (N. Y.) 21, 40–50. https://doi.org/10.1099/00221287-21-1-40.

Dabes, J.N., Finn, R.K., Wilke, C.R., 1973. Equations of substrate-limited growth: the case for blackman kinetics. Biotechnol. Bioeng. 15, 1159–1177. https://doi.org/10.1002/bit.260150613.

Dang, J.S., Harvey, D.M., Jobbagy, A., Grady, C.L., 1989. Evaluation of biodegradation kinetics with respirometric data. Res. J. Water Pollut. Contr. Fed. 1711–1712.

Deb, K., Jain, H., 2014. An evolutionary many-objective optimization algorithm using reference-point-based nondominated sorting approach, Part I: solving problems with box constraints. IEEE Trans. Evol. Comput. 18, 577–601. https://doi.org/10.1109/TEVC.2013.2281535.

Doran, P.M., 1995. Bioprocess Engineering Principles. Academic Press.

Dziga, D., Wladyka, B., Zielińska, G., Meriluoto, J., Wasylewski, M., 2012. Heterologous expression and characterisation of microcystinase. Toxicon 59, 578–586. https://doi.org/10.1016/j.toxicon.2012.01.001.

Edwards, C., Lawton, L.A., 2009. Bioremediation of cyanotoxins. In: Laskin, A., Sariaslani, S., Gadd, G. (Eds.), Adv. Appl. Microbiol, vol. 67. Academic Press, pp. 109–129.

Egli, T., 2010. How to live at very low substrate concentration. Water Res., Microb. Ecol. Drinking Water Waste Water Treat. Process. 44, 4826–4837. https://doi.org/10.1016/j.watres.2010.07.023.

Egli, T., 1995. The ecological and physiological significance of the growth of heterotrophic microorganisms with mixtures of substrates. In: Jones, J.G. (Ed.), Adv. Microb. Ecol. Springer US, pp. 305–386. https://doi.org/10.1007/978-1-4684-7724-5_8.

Eleuterio, L., Batista, J.R., 2010. Biodegradation studies and sequencing of microcystin-LR degrading bacteria isolated from a drinking water biofilter and a fresh water lake. Toxicon 55, 1434–1442. https://doi.org/10.1016/j.toxicon.2010.02.020.

El-Naas, M.H., Acio, J.A., El Telib, A.E., 2014. Aerobic biodegradation of BTEX: progresses and prospects. J. Environ. Chem. Eng. 2, 1104–1122. https://doi.org/10.1016/j.jece.2014.04.009.

Esener, A.A., Roels, J.A., Kossen, N.W.F., 1983. Theory and applications of unstructured growth models: kinetic and energetic aspects. Biotechnol. Bioeng. 25, 2803–2841. https://doi.org/10.1002/bit.260251202.

Faust, K., Raes, J., 2012. Microbial interactions: from networks to models. Nat. Rev. Microbiol. 10, 538–550. https://doi.org/10.1038/nrmicro2832.

Francy, D.S., Graham, J.L., Stelzer, E.A., Ecker, C.D., Brady, A.M., 2015. Water Quality, Cyanobacteria, and Environmental Factors and Their Relations to Microcystin Concentrations for Use in Predictive Models at Ohio Lake Erie and Inland Lake Recreational Sites, 2013-14 (Scientific Investigations Report No. 2015–5120). United States Geological Survey.

Fredrickson, A.G., Ramkrishna, D., Tsuchiya, H.M., 1971. The necessity of including structure in mathematical models of unbalanced microbial growth. Chem. Eng. Symp. Ser. 67, 53–59.

Geisser, S., Eddy, W.F., 1979. A predictive approach to model selection. J. Am. Stat. Assoc. 74, 153–160. https://doi.org/10.1080/01621459.1979.10481632.

Gelman, A., Carlin, J., Stern, H., Vehtari, A., Dunson, D.B., Rubin, D.B., 2014. Bayesian Data Analysis, third ed. CRC Press, Boco Raton, FL.

Grady, C.P.L., Smets, B.F., Barbeau, D.S., 1996. Variability in kinetic parameter estimates: a review of possible causes and a proposed terminology. Water Res. 30, 742–748. https://doi.org/10.1016/0043-1354(95)00199-9.

Gupta, H., Razavi, S., 2017. Chapter 20 - challenges and future outlook of sensitivity analysis. In: Petropoulos, G.P., Srivastava, P.K. (Eds.), Sensitivity Analysis in Earth Observation Modelling. Elsevier, pp. 397–415. https://doi.org/10.1016/B978-0-12-803011-0.00020-3.

Heijnen, J.J., Romein, B., 1995. Derivation of kinetic equations for growth on single substrates based on general properties of a simple metabolic network. Biotechnol. Prog. 11, 712–716. https://doi.org/10.1021/bp00036a018.

Heitzer, A., Kohler, H.P., Reichert, P., Hamer, G., 1991. Utility of phenomenological models for describing temperature dependence of bacterial growth. Appl. Environ. Microbiol. 57, 2656–2665.

Ho, L., Gaudieux, A.-L., Fanok, S., Newcombe, G., Humpage, A.R., 2007. Bacterial degradation of microcystin toxins in drinking water eliminates their toxicity. Toxicon 50, 438–441. https://doi.org/10.1016/j.toxicon.2007.03.021.

Ho, L., Sawade, E., Newcombe, G., 2012. Biological treatment options for cyanobacteria metabolite removal – a review. Water Res., Cyanobacteria: Impacts of Climate Change Occur. Toxicity Water Qual. Manage. 46, 1536–1548. https://doi.org/10.1016/j.watres.2011.11.018.

Holmberg, A., 1982. On the practical identifiability of microbial growth models incorporating Michaelis-Menten type nonlinearities. Math. Biosci. 62, 23–43. https://doi.org/10.1016/0025-5564(82)90061-X.

Huisman, J., Matthijs, H.C.P., Visser, P.M., 2006. Harmful Cyanobacteria. Springer Science & Business Media.

Kim, D., Chung, S., Lee, S., Choi, J., 2012. Relation of microbial biomass to counting units for Pseudomonas aeruginosa. AJMR (Am. J. Ment. Retard.) 6, 4620–4622. https://doi.org/10.5897/AJMR10.902.

Knightes, C.D., Peters, C.A., 2003. Aqueous phase biodegradation kinetics of 10 PAH compounds. Environ. Eng. Sci. 20, 207–218. https://doi.org/10.1089/109287503321671410.

Knightes, C.D., Peters, C.A., 2000. Statistical analysis of nonlinear parameter estimation for monod biodegradation kinetics using bivariate data. Biotechnol. Bioeng. 69, 160–170 https://doi.org/10.1002/(SICI)1097-0290(20000720)69:2<160:AID-BIT5>3.0.CO;2-J.

Koch, A.L., 1982. Multistep kinetics: choice of models for the growth of bacteria. J. Theor. Biol. 98, 401–417. https://doi.org/10.1016/0022-5193(82)90127-8.

Kovárová, K., Zehnder, A.J., Egli, T., 1996. Temperature-dependent growth kinetics of Escherichia coli ML 30 in glucose-limited continuous culture. J. Bacteriol. 178, 4530–4539. https://doi.org/10.1128/jb.178.15.4530-4539.1996.

Kovárová-Kovar, K., Egli, T., 1998. Growth kinetics of suspended microbial cells: from single-substrate-controlled growth to mixed-substrate kinetics. Microbiol. Mol. Biol. Rev. 62, 646–666.

Kruschke, J.K., 2013. Bayesian estimation Supersedes the t test. J. Exp. Psychol. Gen. 142, 573–603. https://doi.org/10.1037/a0029146.

Kruschke, J.K., 2011. Bayesian assessment of null values via parameter estimation and model comparison. Perspect. Psychol. Sci. 6, 299–312. https://doi.org/10.1177/1745691611406925.

Laloy, E., Vrugt, J.A., 2012. High dimensional posterior exploration of hydrologic models using multiple try DREAM(ZS) and high performance computing. Water Resour. Res. 48, W01526. https://doi.org/10.1029/201.1WR010608.

Lauderdale, C., Chadik, P., Kirisits, M.-J., Brown, J., 2012. Engineered biofiltration: enhanced biofilter performance through nutrient and peroxide addition. J. Am. Water Works Assoc. 104, 298–309.

Li, J., Shimizu, K., Akasako, H., Lu, Z., Akiyama, S., Goto, M., Utsumi, M., Sugiura, N., 2015. Assessment of the factors contributing to the variations in microcystins biodegradability of the biofilms on a practical biological treatment facility. Bioresour. Technol. 175, 463–472. https://doi.org/10.1016/j.biortech.2014.10.047.

Li, J., Shimizu, K., Maseda, H., Lu, Z., Utsumi, M., Zhang, Z., Sugiura, N., 2012. Investigations into the biodegradation of microcystin-LR mediated by the biofilm in wintertime from a biological treatment facility in a drinking-water treatment plant. Bioresour. Technol. 106, 27–35. https://doi.org/10.1016/j.biortech.2011.11.099.

Li, J., Shimizu, K., Sakharkar, M.K., Utsumi, M., Zhang, Z., Sugiura, N., 2011. Comparative study for the effects of variable nutrient conditions on the biodegradation of microcystin-LR and concurrent dynamics in microcystin-degrading gene abundance. Bioresour. Technol. 102, 9509–9517. https://doi.org/10.1016/j.biortech.2011.07.112.

Li, Jieming, Li, R., Li, Ji, 2017. Current research scenario for microcystins biodegradation – a review on fundamental knowledge, application prospects and challenges. Sci. Total Environ. 595, 615–632. https://doi.org/10.1016/j.scitotenv.2017.03.285.

Liu, C., Zachara, J.M., 2001. Uncertainties of monod kinetic parameters nonlinearly estimated from batch experiments. Environ. Sci. Technol. 35, 133–141. https://doi.org/10.1021/es001261b.

Manheim, D.C., Detwiler, R., 2018. Accurate and Reliable Estimation of Kinetic

Parameters for Environmental Engineering Applications: a Global, Multi Objective, Bayesian Optimization Approach. MethodsX, (in press).

Mara, T.A., Tarantola, S., Annoni, P., 2015. Non-parametric methods for global sensitivity analysis of model output with dependent inputs. Environ. Model. Software 72, 173–183. https://doi.org/10.1016/j.envsoft.2015.07.010.

McGraw, K.O., Wong, S.P., 1992. A common language effect size statistic. Psychol. Bull. 111, 361–365. https://doi.org/10.1037/0033-2909.111.2.361.

McKie, M.J., Taylor-Edmonds, L., Andrews, S.A., Andrews, R.C., 2015. Engineered biofiltration for the removal of disinfection by-product precursors and genotoxicity. Water Res. 81, 196–207. https://doi.org/10.1016/j.watres.2015.05.034.

Merel, S., Walker, D., Chicana, R., Snyder, S., Baurès, E., Thomas, O., 2013. State of knowledge and concerns on cyanobacterial blooms and cyanotoxins. Environ. Int. 59, 303–327. https://doi.org/10.1016/j.envint.2013.06.013.

Monod, J., 1949. The growth of bacterial cultures. Annu. Rev. Microbiol. 3.

Moser, H., 1958. The Dynamics of Bacterial Populations Maintained in the Chemostat. Carnegie Institution of Washington.

Myers, J.A., Curtis, B.S., Curtis, W.R., 2013. Improving accuracy of cell and chromophore concentration measurements using optical density. BMC Biophys. 6, 4. https://doi.org/10.1186/2046-1682-6-4.

Nihtilä, M., Virkkunen, J., 1977. Practical identifiability of growth and substrate consumption models. Biotechnol. Bioeng. 19, 1831–1850. https://doi.org/10.1002/bit.260191208.

Noel, J.T., Narang, A., 2009. Gene regulation in continuous cultures: a unified theory for bacteria and yeasts. Bull. Math. Biol. 71, 453–514. https://doi.org/10.1007/s11538-008-9369-3.

Okpokwasili, G.C., Nweke, C.O., 2006. Microbial growth and substrate utilization kinetics. Afr. J. Biotechnol. 5, 305–317.

O'Neil, J.M., Davis, T.W., Burford, M.A., Gobler, C.J., 2012. The rise of harmful cyanobacteria blooms: the potential roles of eutrophication and climate change. Harmful Algae, Harmful Algae–The requirement for species-specific information 14, 313–334. https://doi.org/10.1016/j.hal.2011.10.027.

Paerl, H.W., Huisman, J., 2009. Climate change: a catalyst for global expansion of harmful cyanobacterial blooms. Environ. Microbiol. Rep. 1, 27–37. https://doi.org/10.1111/j.1758-2229.2008.00004.x.

Paerl, H.W., Paul, V.J., 2012. Climate change: links to global expansion of harmful cyanobacteria. Water Res., Cyanobacteria: Impacts Climate Change Occur. Toxicity Water Qual. Manage. 46, 1349–1363. https://doi.org/10.1016/j.watres.2011.08.002.

Panikov, N., 1995. Microbial Growth Kinetics, first ed. Chapman & Hall, London, United Kingdom.

Panikov, N., Pirt, S.J., 1978. The effects of cooperativity and growth yield variation on the kinetics of nitrogen or phosphate limited growth of *chlorella* in a chemostat culture. Microbiology (N. Y.) 108, 295–303. https://doi.org/10.1099/00221287-108-2-295.

Powell, E.O., 1967. The growth of microorganisms as a function of substrate concentration. In: Evans, C.G.T., Strange, R.E., Tempest, D.W. (Eds.), Microbial Physiology and Continuous Culture. HMSO, London, United Kingdom.

Puddick, J., Prinsep, M.R., Wood, S.A., Kaufononga, S.A.F., Cary, S.C., Hamilton, D.P., 2014. High levels of structural diversity observed in microcystins from Microcystis CAWBG11 and characterization of six new microcystin congeners. Mar. Drugs 12, 5372–5395. https://doi.org/10.3390/md12115372.

Ramkrishna, D., Fredrickson, A.G., Tsuchiya, H.M., 1967. Dynamics of microbial propagation: models considering inhibitors and variable cell composition. Biotechnol. Bioeng. 9, 129–170. https://doi.org/10.1002/bit.260090203.

Razavi, S., Gupta, H.V., 2016a. A new framework for comprehensive, robust, and efficient global sensitivity analysis: 1. Theory. Water Resour. Res. 52, 423–439. https://doi.org/10.1002/2015WR017558.

Razavi, S., Gupta, H.V., 2016b. A new framework for comprehensive, robust, and efficient global sensitivity analysis: 2. Application. Water Resour. Res. 52, 440–455. https://doi.org/10.1002/2015WR017559.

Razavi, S., Gupta, H.V., 2015. What do we mean by sensitivity analysis? The need for comprehensive characterization of “global” sensitivity in Earth and Environmental systems models. Water Resour. Res. 51, 3070–3092. https://doi.org/10.1002/2014WR016527.

Reardon, K.F., Mosteller, D.C., Bull Rogers, J.D., 2000. Biodegradation kinetics of benzene, toluene, and phenol as single and mixed substrates for *Pseudomonas putida F1*. Biotechnol. Bioeng. 69, 385–400 https://doi.org/10.1002/1097-0290(20000820)69:4<385:AID-BIT5>3.0.CO;2-Q.

Reardon, K.F., Mosteller, D.C., Rogers, J.B., DuTeau, N.M., Kim, K.-H., 2002. Biodegradation kinetics of aromatic hydrocarbon mixtures by pure and mixed bacterial cultures. Environ. Health Perspect. 110, 1005–1011.

Rittmann, B.E., Crawford, L., Tuck, C.K., Namkung, E., 1986. In situ determination of kinetic parameters for biofilms: isolation and characterization of oligotrophic biofilms. Biotechnol. Bioeng. 28, 1753–1760. https://doi.org/10.1002/bit.260281120.

Rittmann, B.E., Stilwell, D., Ohashi, A., 2002. The transient-state, multiple-species biofilm model for biofiltration processes. Water Res. 36, 2342–2356. https://doi.org/10.1016/S0043-1354(01)00441-9.

Robinson, J.A., 1985. Determining microbial kinetic parameters using nonlinear regression analysis. In: Advances in Microbial Ecology, Adv. Microb. Ecol. Springer, Boston, MA, pp. 61–114. https://doi.org/10.1007/978-1-4615-9412-3_2.

Robinson, J.A., Tiedje, J.M., 1983. Nonlinear estimation of Monod growth kinetic parameters from a single substrate depletion curve. Appl. Environ. Microbiol. 45, 1453–1458.

Rosso, L., Lobry, J.R., Bajard, S., Flandrois, J.P., 1995. Convenient model to describe the combined effects of temperature and pH on microbial growth. Appl. Environ. Microbiol. 61, 610–616.

Rosso, L., Lobry, J.R., Flandrois, J.P., 1993. An unexpected correlation between cardinal temperatures of microbial growth highlighted by a new model. J. Theor. Biol. 162, 447–463. https://doi.org/10.1006/jtbi.1993.1099.

Sadegh, M., Vrugt, J.A., 2014. Approximate bayesian computation using Markov chain Monte Carlo simulation: DREAM(ABC). Water Resour. Res. 50, 6767–6787. https://doi.org/10.1002/2014WR015386.

Saltelli, A., Ratto, M., Andres, T., Campolongo, F., Cariboni, J., Gatelli, D., Saisana, M., Tarantola, S., 2008. Global Sensitivity Analysis: the Primer. John Wiley & Sons.

Schmidt, J.R., Wilhelm, S.W., Boyer, G.L., 2014. The fate of microcystins in the environment and challenges for monitoring. Toxins 6, 3354–3387. https://doi.org/10.3390/toxins6123354.

Shuler, M.L., Kargi, F.K., 2002. Bioprocess Engineering: Basic Concepts. Prentice Hall, Upper Saddle River, NJ, USA.

Simkins, S., Alexander, M., 1984. Models for mineralization kinetics with the variables of substrate concentration and population density. Appl. Environ. Microbiol. 47, 1299–1306.

Song, H.-S., Cannon, W.R., Beliaev, A.S., Konopka, A., 2014. Mathematical modeling of microbial community dynamics: a methodological review. Processes 2, 711–752. https://doi.org/10.3390/pr2040711.

Suarez, M.P., Rifai, H.S., 1999. Biodegradation rates for fuel hydrocarbons and chlorinated solvents in groundwater. Biorem. J. 3, 337–362. https://doi.org/10.1080/10889869991219433.

Tchobanoglous, G., Burton, F.L., Stensel, H.D., 2003. Wastewater Engineering: Treatment and Reuse, fourth ed. McGraw Hill, New York, NY.

Tessier, G., 1942. Croissance des populations bactériennes et quantité d'aliment disponible. Rev. Sci. Paris 80.

Tyagi, M., Fonseca, M.M.R. da, Carvalho, C.C.C.R. de, 2010. Bioaugmentation and biostimulation strategies to improve the effectiveness of bioremediation processes. Biodegradation 22, 231–241. https://doi.org/10.1007/s10532-010-9394-4.

U.S. EPA, 2015. Drinking water health advisory for the cyanobacterial microcystin toxins (No. 820R15100.). https://www.epa.gov/sites/production/files/2017-06/documents/microcystins-report-2015.pdf. (Accessed 30 March 2018).

Valeria, A.M., Ricardo, E.J., Stephan, P., Alberto, W.D., 2006. Degradation of microcystin-RR by *Sphingomonas sp.* CBA4 isolated from san roque reservoir (córdoba – Argentina). Biodegradation 17, 447–455. https://doi.org/10.1007/s10532-005-9015-9.

Velten, S., Hammes, F., Boller, M., Egli, T., 2007. Rapid and direct estimation of active biomass on granular activated carbon through adenosine triphosphate (ATP) determination. Water Res. 41, 1973–1983. https://doi.org/10.1016/j.watres.2007.01.021.

Velten, S., Boller, M., Koster, O., Helbing, J., Weilenmann, H.U., Hammes, F., 2011. Development of biomass in a drinking water granular active carbon (GAC) filter. Water Res. 45, 6347–6354. https://doi.org/10.1016/j.watres.2011.09.017.

Vrugt, J.A., Robinson, B.A., Hyman, J.M., 2009. Self-adaptive multimethod search for global optimization in real-parameter spaces. IEEE Trans. Evol. Comput. 13, 243–259. https://doi.org/10.1109/TEVC.2008.924428.

Wang, J., Wu, P., Chen, J., Yan, H., 2010. Biodegradation of microcystin-RR by a new isolated *Sphingopyxis sp.* USTB-05. Chin. J. Chem. Eng. 18, 108–112. https://doi.org/10.1016/S1004-9541(08)60330-4.

Westrick, J.A., 2008. Cyanobacterial toxin removal in drinking water treatment processes and recreational waters. In: Hudnell, H.K. (Ed.), Cyanobacterial Harmful Algal Blooms: State of the Science and Research Needs, Adv. Exp. Med. Biol. Springer, New York, pp. 275–290. https://doi.org/10.1007/978-0-387-75865-7_13.

Westrick, J.A., Szlag, D.C., Southwell, B.J., Sinclair, J., 2010. A review of cyanobacteria and cyanotoxins removal/inactivation in drinking water treatment. Anal. Bioanal. Chem. 397, 1705–1714. https://doi.org/10.1007/s00216-010-3709-5.

Wöhling, T., Vrugt, J.A., Barkle, G.F., 2008. Comparison of three multiobjective optimization algorithms for inverse modeling of vadose zone hydraulic properties. Soil Sci. Soc. Am. J. 72, 305–319. https://doi.org/10.2136/sssaj2007.0176.

Xiao, C., Yan, H., Wang, J., Wei, W., Ning, J., Pan, G., 2011. Microcystin-lr biodegradation by Sphingopyxis sp. USTB-05. Front. Environ. Sci. Eng. China 5, 526–532. https://doi.org/10.1007/s11783-010-0261-7.

Yoon, H., Klinzing, G., Blanch, H.W., 1977. Competition for mixed substrates by microbial populations. Biotechnol. Bioeng. 19, 1193–1210. https://doi.org/10.1002/bit.260190809.

Zhang, J., Shi, H., Liu, A., Cao, Z., Hao, J., Gong, R., 2015. Identification of a new microcystin-degrading bacterium isolated from lake chaohu, China. Bull. Environ. Contam. Toxicol. 94, 661–666. https://doi.org/10.1007/s00128-015-1531-7.